Millimeter-Wave Base Station Deployment Using the Scenario Sampling Approach

Miaomiao Dong, Taejoon Kim, *Senior Member, IEEE*, Jingjin Wu, *Member, IEEE*, and Eric Wing-Ming Wong, *Senior Member, IEEE*

***Abstract*—While the Poisson point process (PPP) has been widely employed to model the user distribution in many network design problems, an existing challenge is that it often reveals inaccuracy in small-cell networks. In this paper, instead of employing PPP, we capture the randomness of user equipment (UE) by collecting many their realizations. Specifically, we focus on the millimeter-wave (mmWave) base station (BS) deployment problem in an urban geometry, based on the application of a scenario sampling approach, previously introduced for large-scale optimization, to quantitatively sample a portion of the UE realizations. Motivated by the scenario sampling, a reduced-scale mmWave BS deployment problem is formulated, whose optimal solution is attained by the proposed low-complexity iterative search algorithm. A required number of samples that guarantee a specified majority of the link quality constraints is analyzed. Simulation results verify the scenario sampling theory and the effectiveness of the proposed algorithm.**

***Index Terms*—Millimeter-wave networks, base station deployment, scenario sampling, large-scale integer linear programming.**

I. Introduction

The ever-growing number of high data rate mobile applications coupled with the promise of connecting billions of user equipments (UEs) is demanding the deployment of millimeter-wave (mmWave) small-cell networks at large scale. Due to the high frequency and directional transmission, millimeter wave (mmWave) links are less susceptible to interference but are more vulnerable to physical blockage caused by obstacles in urban geometry [1]. Moreover, the capacity of each mmWave base station (BS),[1] equipped with hybrid antenna arrays, is strictly limited by the number of radio frequency (RF) chains, in which capacity-limited blockage occurs when all RF chains are occupied by user equipments (UEs).

To mitigate both the physical and capacity-limited blockages, multiple BSs can be installed to cover a region. The more the number of deployed BSs, the more UEs can be served with reduced blockages. However, deploying more BSs comes at the price of higher network deployment and maintenance costs. To mitigate this issue, cost-efficient approaches that minimize the number of deployed BSs while keeping the outage of each UE below a certain threshold, has been considered more recently [2], [3]. However, solution approaches to the latter problems largely depend on the UE deployment statistics in the geometry of interest [4]. While the Poisson point process (PPP) was validated for macro-cellular networks to capture the randomness of UEs, it often reveals inaccuracy in the small-cell dense mmWave networks [5]. Holding both the accuracy and tractability of a stochastic model is often a dilemma because geometry-dependency exponentially adds complexity to network design problems. It is within this context that in the mmWave BS deployment literature, the UE distribution is often ignored [6], [7] or many simplifying assumptions have been made [2], [3]. An alternative approach is to rely on available UE realization data that have been measured at different time scales to sufficiently capture the randomness of UEs.[2] Although a major benefit of leveraging the measurement data is its accuracy, involving all realizations to solve the BS deployment problem is yet computationally prohibitive.

In this work, we propose a scenario sampling approach, previously studied in the context of large-scale convex problems [9] to solve the blockage probability-guaranteed minimum-cost mmWave BS deployment problem in an urban geometry. For each UE realization, we analyze the physical and capacity-limited blockage probabilities and formulate the mmWave BS deployment into a large-scale integer linear problem (ILP), which is non-convex and excessively complex to be directly solved. The scenario sampling approach is then applied to form a small-scale ILP. The global optimality of the samll-scale ILP is achieved by the proposed low-complexity iterative search algorithm. However, any domain reduction introduced by the sampling could lead to substantial suboptimality. Thus, a required number of samples that ensure the optimal solution of the reduced problem satisfies a specified majority of the UE realizations is derived. We perform numerical simulations to corroborate the established analysis as well as effectiveness of the proposed algorithm.

It should be noted that the mmWave BS deployment problem in this work is approached in a link-connectivity point-of-view with the primary focus on providing the initial connectivity to UEs with the blockage tolerance guarantees. Therefore, our major focus is not to describe a physical-layer algorithmic approach for the quality-of-service improvement that can be readily implemented, after the BS deployment, by leveraging existing directional beam optimization and power allocation techniques [10] or investigating new ways of enhancing such techniques, which is subject to further research and not the focus of the present work.

The rest of the work is organized as follows. In Section II, we describe the mmWave BS deployment scenario under consideration and contrive the blockage constraints. Section III formulates the mmWave BS deployment into a large-scale ILP, which is further reduced to be a small-scale ILP by using the scenario sampling approach in Section IV. The small-scale ILP is optimally solved in Section V. Simulation verification and conclusions are given in Section VI and VII, respectively.

Manuscript received March 2, 2020; revised September 3, 2020; accepted September 8, 2020. Date of publication September 23, 2020; date of current version November 12, 2020. The work was supported in part by the Innovation and Technology Fund of the Hong Kong Special Administrative Region, China under Grant ITS/359/17. The work of Taejoon Kim was supported by the National Science Foundation (NSF) under under CNS 1955561 and AST 2037864. The work of Jingjin Wu was supported by BNU-HKBU UIC College Research under Grants 201811 and 201911. The review of this article was coordinated by Prof. Dania Marabissi. *(Corresponding author: Eric Wing-Ming Wong.)*

Miaomiao Dong and Eric Wing-Ming Wong are with the Department of Electrical Engineering, City University of Hong Kong, Hong Kong (e-mail: miao4600@163.com; eeewong@cityu.edu.hk).

Taejoon Kim is with the Department of Electrical Engineering and Computer Science, University of Kansas, Lawrence, KS 66045 USA (e-mail: taejoonkim@ku.edu).

Jingjin Wu is with the Department of Statistics, BNU-HKBU United International College, Zhuhai, Guangdong 519087, China (e-mail: jj.wu@ieee.org).

Digital Object Identifier 10.1109/TVT.2020.3026216

[1]BS capacity refers to the maximum number of UEs that a BS can simultaneously serve.

[2]For example, UE placements in a network can be collected by the existing LTE BSs using positioning reference signals as described in [8].

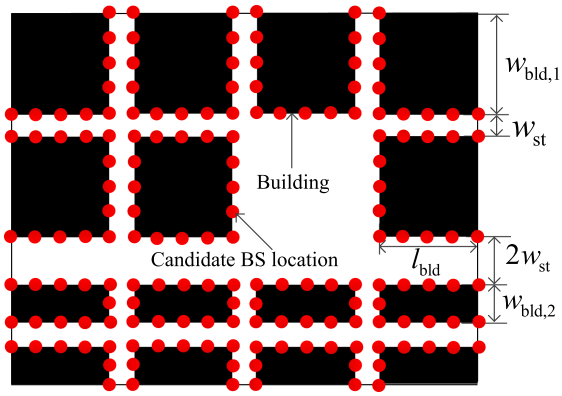

Fig. 1. Urban street geometry for mmWave BS deployment with $B = 164$ candidate locations.

II. System Setup

We consider an urban street geometry, as shown in Fig. 1,[3] consisting of rectangular buildings with length l_{bld} and width $w_{\text{bld},1}$ and $w_{\text{bld},2}$. These buildings are separated by streets with width w_{st} and $2w_{\text{st}}$. The outdoor BSs can be wall-mounted at the candidate locations, i.e., red dots at the boundaries of each building in Fig. 1, indexed by $b \in \mathcal{B} = \{1, 2, \ldots, B\}$. We assume that B is an even integer throughout the paper. A column vector $\mathbf{y} = [y_1, y_2, \ldots, y_B]^T$ is employed to denote the state of each BS candidate location. If a BS is deployed at the bth location, we set $y_b = 1$, and $y_b = 0$ otherwise. A candidate location can be occupied by at most one BS to serve outdoor UEs distributed on streets. We shall use "BS b" to denote the BS deployed at the bth candidate location. Let Δ be the set of measured active UE realizations with the cardinality $\text{card}(\Delta) = K$, where K can be very large, depending on the time scale. Given a realization $\delta \in \Delta$, we denote the number of active UEs in δ as $U^{(\delta)}$ and their locations are known.

Because non-line-of-sight (NLoS) mmWave links suffer from much larger attenuation than LoS links, we only take the LoS paths into account for the BS deployment at 28 GHz mmWave bands, while neglecting the NLoS paths. These LoS paths can be occasionally blocked by random obstacles (e.g., vehicles and pedestrians) on streets in Fig. 1. By modeling the random obstacles using a Boolean scheme, blockage probability of the LoS link [12] between BS b and UE u in a $\delta \in \Delta$ can be modeled by

$$p_{u,b}^{(\delta),\text{blk}}(r_{u,b}) = 1 - \exp(-\beta r_{u,b} - \alpha), \tag{1}$$

where $r_{u,b}$ is the link distance between BS b and UE u, and $\alpha > 0$ and $\beta > 0$ are the parameters that depend on the density and sizes of the random obstacles, respectively. The larger the density and sizes of obstacles, the bigger the values of α and β are, resulting in higher $p_{u,b}^{(\delta),\text{blk}}(r_{u,b})$. Because sizes of the random obstacles are usually much smaller than the link distance, we assume independent link blockage [12], [13]. Under these assumptions, in what follows, we analyze physical and capacity-limited blockage probabilities to be adopted to BS deployment problem formulation in Section III.

[3]While the urban geometry in Fig. 1 originates from the METIS project [11, Fig. B-2], the devised approach in this paper can be directly applied to any geometry with pre-determined candidate BS locations.

A. Physical Blockage

We define $N_b^{(\delta)} \leq U^{(\delta)}$ as the number of the nearest active UEs that can be served by BS b in realization $\delta \in \Delta$. An indicator $\Lambda_{u,b}^{(\delta)}(N_b^{(\delta)})$ is introduced such that $\Lambda_{u,b}^{(\delta)}(N_b^{(\delta)}) = 1$ implies that UE u in $\delta \in \Delta$ can be served by BS b, and $\Lambda_{u,b}^{(\delta)}(N_b^{(\delta)}) = 0$, otherwise. Thus, $y_b \Lambda_{u,b}^{(\delta)}(N_b^{(\delta)}) = 1$ implies that the UE u in δ is served by BS b. In the context of mmWave BS deployment, we allow for multiple BSs to simultaneously serve an active UE of interest to combat physical blockages, i.e., mathematically,

$$\sum_b y_b \Lambda_{u,b}^{(\delta)}(N_b^{(\delta)}) \geq 1.$$

Then, a physical outage can be defined as an event that the links from all BSs covering a UE are blocked by random obstacles on the streets. Provided the independent blockage assumption, the physical blockage constraint is formulated as

$$\sum_{b=1}^{B} y_b \Lambda_{u,b}^{(\delta)}(N_b^{(\delta)}) \log\left(p_{u,b}^{(\delta),\text{blk}}\right) \leq \log\left(\zeta^{\text{phy}}\right), \quad \forall u \in \mathcal{U}^{(\delta)}, \tag{2}$$

where $\mathcal{U}^{(\delta)}$ is the index set of the $U^{(\delta)}$ active UEs, i.e., $\text{card}(\mathcal{U}^{(\delta)}) = U^{(\delta)}$, and ζ^{phy} is the physical blockage tolerance level. We let $\mathbf{A}^{(\delta)}(\mathbf{N}^{(\delta)}) \in \mathbb{R}^{U^{(\delta)} \times B}$ be a matrix with the entry $\Lambda_{u,b}^{(\delta)}(N_b^{(\delta)}) \log(p_{u,b}^{(\delta),\text{blk}})$ at the uth row and bth column, and $\mathbf{b} \in \mathbb{R}^{U^{(\delta)} \times 1}$ be a column vector with each entry $\log(\zeta^{\text{phy}})$, where $\mathbf{N}^{(\delta)} = [N_1^{(\delta)}, \ldots, N_B^{(\delta)}]$. A compact form of (2) is

$$\mathbf{A}^{(\delta)}\left(\mathbf{N}^{(\delta)}\right) \mathbf{y} \preceq \mathbf{b}, \tag{3}$$

where $\preceq$ represents the entry-wise less than or equal to.

B. Capacity-Limited Blockage

As discussed in Section I, BS capacity is limited by the number of RF chains N_{RF}. If $N_b^{(\delta)} \leq N_{\text{RF}}$, no capacity-limited blockages occurs. On the other hand, if $N_b^{(\delta)} > N_{\text{RF}}$, the capacity-limited blockage could occur if the number of physically-blocked UEs is less than $N_b^{(\delta)} - N_{\text{RF}}$. Thus, the probability of the capacity-limited blockage can be written as

$$f\left(N_b^{(\delta)}\right) = 1_{N_b^{(\delta)} > N_{\text{RF}}} \sum_{i=0}^{N_b^{(\delta)} - N_{\text{RF}} - 1} \sum_{j=1}^{\binom{N_b^{(\delta)}}{i}} q_{i,j}^{(\delta)}, \tag{4}$$

where $1_{N_b^{(\delta)} > N_{\text{RF}}} = 1$ if $N_b^{(\delta)} > N_{\text{RF}}$, and $1_{N_b^{(\delta)} > N_{\text{RF}}} = 0$, otherwise. The index i denotes the number of physically-blocked UEs and $q_{i,j}^{(\delta)}$ is the probability of i physically-blocked UEs in the jth combination in (4)

$$q_{i,j}^{(\delta)} = \prod_{u \in \Phi_{i,j}} p_{u,b}^{(\delta),\text{blk}} \prod_{u \in \mathcal{N}_b^{(\delta)} - \Phi_{i,j}} \left(1 - p_{u,b}^{(\delta),\text{blk}}\right),$$

where $\mathcal{N}_b^{(\delta)}$ is the index set of the nearest $N_b^{(\delta)}$ UEs in realization δ, and $\Phi_{i,j} \subset \mathcal{N}_b^{(\delta)}$ is the index set of the i physically-blocked UEs in the jth combination in (4). The capacity-limited blockage constraint is thus formulated by

$$f\left(N_b^{(\delta)}\right) \leq \zeta^{\text{cap}}, \quad \forall b \in \mathcal{B}, \forall \delta \in \Delta, \tag{5}$$

where ζ^{cap} is the capacity-limited blockage tolerance level.

III. BS Deployment Problem

The aimed mmWave BS deployment problem is given by

$$\min_{\mathbf{y},\mathbf{N}^{(\delta)}} \quad \sum_{b=1}^{B} y_b \tag{6}$$

$$\text{subject to:} \quad f(N_b^{(\delta)}) \le \zeta^{\text{cap}}, \qquad \forall b \in \mathcal{B}, \forall \delta \in \Delta, \tag{7}$$

$$\mathbf{A}^{(\delta)}\left(\mathbf{N}^{(\delta)}\right)\mathbf{y} \preceq \mathbf{b}, \quad \forall \delta \in \Delta. \tag{8}$$

It optimizes the BS deployment vector $\mathbf{y}$ and UE distribution $\mathbf{N}^{(\delta)}$ to minimize the number of deployed BSs subject to the capacity-limited and physical blockage constraints.

The monotonicity of $f(N_b^{(\delta)})$ and $\mathbf{A}^{(\delta)}(\mathbf{N}^{(\delta)})\mathbf{y}$ with $N_b^{(\delta)}$ in (7) and (8), respectively, leads to the following lemma.

Lemma 1: Suppose the problem in (6) is feasible. Then, the optimal solution $(\mathbf{y}_\Delta^\star, \mathbf{N}^{(\delta)\star})$ to (6) is attained if each entry of $\mathbf{N}^{(\delta)\star}$ is the maximum $N_b^{(\delta)}$ satisfying (7), $\forall b \in \mathcal{B}$, $\forall \delta \in \Delta$.

Proof: It is evident from (2) that as $\sum_{b=1}^{B} y_b \Lambda_{u,b}^{(\delta)}(N_b^{(\delta)})$ increases, the left-hand-side (LHS) of (2) decreases. This implies, as $N_b^{(\delta)}$ grows, each entry on the LHS of (8) decreases, making the physical blockage constraint further feasible (relaxation). On the other hand, the LHS of (7) is an increasing function of $N_b^{(\delta)}$. Thus, the maximum $N_b^{(\delta)}$ of (6), which is also feasible, is determined by (7). Suppose that for any feasible solution $(\mathbf{y}_\Delta, \mathbf{N}^{(\delta)})$ to (6), where some elements in $\mathbf{N}^{(\delta)}$ are not their maximum possible values, we increase these elements to their maximum and obtain another feasible solution $(\mathbf{y}_\Delta, \widetilde{\mathbf{N}}^{(\delta)})$. Then, the pair $(\mathbf{y}_\Delta, \widetilde{\mathbf{N}}^{(\delta)})$ achieves a lower objective in (6) than $(\mathbf{y}_\Delta, \mathbf{N}^{(\delta)})$ because the constraints in (8) become further relaxed. This verifies that the optimal $\mathbf{y}_\Delta^\star$ should be attained by $\widetilde{\mathbf{N}}^{(\delta)}$, which completes the proof. ■

By Lemma 1, one can find the maximum $N_b^{(\delta)}$ satisfying (7), which is denoted as $\bar{N}_b^{(\delta)}$, by increasing $N_b^{(\delta)}$ from $N_b^{(\delta)} = N_{\text{RF}}$, $\forall b \in \{1, 2, \ldots, B\}$, $\forall \delta \in \Delta$. Thus, substituting $N_b^{(\delta)} = \bar{N}_b^{(\delta)}$, $\forall b \in \{1, 2, \ldots, B\}$, simplifies problem (6) to

$$\min_{\mathbf{y}} \sum_{b=1}^{B} y_b \quad \text{subject to: } \mathbf{A}^{(\delta)}\mathbf{y} \preceq \mathbf{b}, \ \forall \delta \in \Delta. \tag{9}$$

We note that the problem in (9) is a binary ILP. While ILP has been extensively studied and there are efficient solvers (e.g., Gurobi [14]), the significantly increased dimensions of the constraint matrices

$$\mathbf{A} = \left[\left(\mathbf{A}^{(\delta_1)}\right)^T, \left(\mathbf{A}^{(\delta_2)}\right)^T, \ldots, \left(\mathbf{A}^{(\delta_K)}\right)^T\right]^T \in \mathbb{R}^{\sum_{\delta\in\Delta} U^{(\delta)} \times B} \tag{10}$$

in (9) demand a prohibitively large amount of computing power and resources, such as random access memory (RAM), to store and process the matrix $\mathbf{A}$. This issues often causes memory outage, making it impractical to be solved at scale. To address these challenges, we propose the scenario sampling approach in the next section.

IV. Scenario Sampling Approach

We first introduce a set $\mathcal{A}(N) = \{\delta_1, \delta_2, \ldots, \delta_N\}$, obtained by randomly sampling N elements of Δ. Replacing Δ in (9) with the sampled set $\mathcal{A}(N)$ leads to a reduced-scale problem:

$$\min_{\mathbf{y}} \sum_{b=1}^{B} y_b \quad \text{subject to: } \mathbf{A}^{(\delta)}\mathbf{y} \preceq \mathbf{b}, \ \forall \delta \in \mathcal{A}(N). \tag{11}$$

We denote by $\mathbf{y}_{\mathcal{A}(N)}^\star$ the optimal solution to (11). How to determine the number of samples N has profound impact to the effectiveness of the reduced-scale problem in (11) – the number of samples N should be determined so that $\mathbf{y}_{\mathcal{A}(N)}^\star$ is feasible to a specified majority of UE realizations in Δ. Hence, we introduce violation probability of $\mathbf{y}_{\mathcal{A}(N)}^\star$:

$$V\left(\mathbf{y}_{\mathcal{A}(N)}^\star\right) = \Pr\left(\delta \in \Delta, \ \mathbf{A}^{(\delta)}\mathbf{y}_{\mathcal{A}(N)}^\star \not\preceq \mathbf{b}\right). \tag{12}$$

Definition 1: We say a solution $\mathbf{y}_{\mathcal{A}(N)}^\star$ is robust if $V(\mathbf{y}_{\mathcal{A}(N)}^\star) \le \epsilon$, where $\epsilon > 0$ is an arbitrary small value.

Note here that a different $\mathcal{A}(N)$ in (11) results in a different optimal solution $\mathbf{y}_{\mathcal{A}(N)}^\star$ and different violation probability $V(\mathbf{y}_{\mathcal{A}(N)}^\star)$. We let

$$\mathcal{B} = \left\{\mathcal{A}(N) = (\delta_1, \delta_2, \ldots, \delta_N), V\left(\mathbf{y}_{\mathcal{A}(N)}^\star\right) > \epsilon\right\} \tag{13}$$

be a set consisting of $\{\mathcal{A}(N)\}$, with which the solution $\mathbf{y}_{\mathcal{A}(N)}^\star$ to (11) becomes nonrobust. Guaranteeing the robustness with probability exceeding $1-\gamma$ requires randomly sampled $\mathcal{A}(N)$s satisfying

$$\Pr(\mathcal{B}) \le \gamma, \tag{14}$$

where $\gamma > 0$ is an arbitrary, small constant. Obviously, as N grows, both $V(\mathbf{y}_{\mathcal{A}(N)}^\star)$ in (12) and $\Pr(\mathcal{B})$ in (14) decrease and, we have

$$V\left(\mathbf{y}_{\mathcal{A}(N)}^\star\right) = \Pr(\mathcal{B}) = 0, \ \text{ if } \ N = \text{card}(\Delta).$$

In what follows, we derive a required number of samples $\overline{N}(\epsilon, \gamma)$ in a sense that any $N \ge \overline{N}(\epsilon, \gamma)$ guarantees (14). Derivations of such a minimum number of samples was originally studied in [9] for convex problems. In this work, we extend this prior work to the ILP in (11), which is non-convex.

A. Preliminaries

We begin by introducing a definition of a *supportive UE realization set*, based on the fact that removing a $\delta \in \mathcal{A}(N)$ from $\mathcal{A}(N)$ either unchanges or decreases the objective function value of (11). In particular, we iteratively remove UE realizations one by one from $\mathcal{A}(N)$ where the $\mathcal{A}(N)$ after the ith omission is denoted as $\mathcal{A}_i(N) \subset \mathcal{A}(N)$. Because $\mathcal{A}_i(N) \subset \mathcal{A}_{i-1}(N)$, after the ith omission, the optimal objective value of (11) either keeps unchanged or decreases. The ith omitted UE realization is said to be *supportive* if the objective function value of (11) is decreased by $s_i > 0$, and it is unsupportive, otherwise. The omission continues until $\mathcal{A}(N)$ becomes empty, i.e., $i = N$.

Definition 2: In a sequential removal of realizations from $\mathcal{A}(N)$, the collection of all supportive UE realizations is called a supportive UE realization set, denoted by $\mathcal{A}_{\text{sup}}$.

Remark 1: An example of a supportive UE realization set is

$$\mathcal{A}_{\text{sup}} = \{\delta_{i_1}, \delta_{i_2}, \ldots, \delta_{i_M}\}, i_m < i_{m+1}, \forall m, \tag{15}$$

where δ_{i_m} is the i_m th omission that is supportive. It is straightforward to conclude that $\text{sum}(\mathbf{y}_{\mathcal{A}(N)}^\star) = \sum_{m=1}^{M} s_{i_m}$, where $\text{sum}(\mathbf{y}_{\mathcal{A}(N)}^\star)$ is the summation of all entries of the optimal solution $\mathbf{y}_{\mathcal{A}(N)}^\star$ to (11). Then, the cardinality of $\mathcal{A}_{\text{sup}}$, $\text{card}(\mathcal{A}_{\text{sup}}) = M$, is no larger than B, i.e., $M \le B$, due to the fact that $\text{sum}(\mathbf{y}_{\mathcal{A}(N)}^\star) = \sum_{m=1}^{M} s_{i_m} \le B$.

Lemma 2: There exist a subset $\mathcal{A}(B) \subset \mathcal{A}(N)$ such that, for $N > B$, any optimal solution to problem (11) is also optimal to the problem:

$$\min_{\mathbf{y}} \sum_{b=1}^{B} y_b \quad \text{subject to: } \mathbf{A}^{(\delta)}\mathbf{y} \preceq \mathbf{b}, \ \forall \delta \in \mathcal{A}(B). \tag{16}$$

Proof: We first note that the ILP in (11) can have multiple optimal solutions and any optimal solution $\mathbf{y}_{\mathcal{A}(N)}^\star$ to (11) is feasible to (16). Thus, it suffices to show that there exists a set $\mathcal{A}(B) \subset \mathcal{A}(N)$ and

the problem (16) under $\mathcal{A}(B) \subset \mathcal{A}(N)$ has the same optimal objective value as (11).

By Remark 1, a set $\mathcal{A}(N)$ with $N > B$ can include at least $N - B$ unsupportive UE realizations. Omitting these unsupportive UE realizations from $\mathcal{A}(N)$ yields $\mathcal{A}(B)$ satisfying

$$\mathcal{A}_{\text{sup}} \subseteq \mathcal{A}(B) \subset \mathcal{A}(N). \tag{17}$$

Consider the omission sequence of the elements in $\mathcal{A}(B)$, in reverse order, that results in the same $\mathcal{A}_{\text{sup}}$ in (17). Initially, we start with evaluating the last supportive realization $\{\delta_{i_M}\}$, for which the optimal objective value of (16) increases from zero to s_{i_M}. Sequentially evaluating UE realization in $\mathcal{A}(B)$, the objective value of (16) is unchanged until the $\delta_{i_{M-1}}$ is added to $\{\delta_{i_M}\}$, yielding the objective $s_{i_{M-1}} + s_{i_M}$. We repeat the above procedures until evaluating all elements in $\mathcal{A}(B)$, in which the optimal objective value of (16) is $\sum_{m=1}^{M} s_{i_m}$. Because the following holds $\text{sum}(\mathbf{y}^{\star}_{\mathcal{A}(N)}) = \sum_{m=1}^{M} s_{i_m}$ by Remark 1, problems (11) and (16) share the same objective value, which completes the proof. ■

B. Required Number of Samples

Evidenced by Lemma 2, all optimal solutions to (11) for an arbitrary $\mathcal{A}(N)$ can be enumerated by counting the optimal solutions to (16). Motivated by this observation, we find a lower bound $\overline{N}(\epsilon, \gamma)$ of the required number of samples that ensures the robustness of (11), which is our main result of this section.

Theorem 1: A lower bound of the number of samples N that guarantees a robust solution to (11) with probability exceeding $1 - \gamma$ is given by

$$\overline{N}(\epsilon, \gamma) = \left\lceil B + \frac{\ln \gamma - (K-B) \ln \frac{K}{K-B} - B \ln \frac{K}{B} - \ln \binom{B}{B/2}}{\ln(1-\epsilon)} \right\rceil, \tag{18}$$

where $\lceil x \rceil$ is the smallest integer larger than or equal to x.

Proof: The ILP in (16) can have multiple optimal solutions. Without loss of generality, we denote the ℓth optimal solution as $\mathbf{y}^{\star}_{\mathcal{A}(B),\ell}$. Then, for any arbitrary $\mathcal{A}(B)$, the number of optimal solutions to (16) is limited by[4]

$$\text{Number of optimal solutions} \leq \binom{B}{\text{sum}\left(\mathbf{y}^{\star}_{\mathcal{A}(B),\ell}\right)} \leq \binom{B}{B/2}. \tag{19}$$

We let a subset of $\mathcal{B}$ in (13) with $\mathbf{y}^{\star}_{\mathcal{A}(N)} = \mathbf{y}^{\star}_{\mathcal{A}(B),\ell}$ be

$$\mathcal{B}_{\mathcal{A}(B),\ell} = \left\{ \mathcal{A}(N) = (\mathcal{A}(B), \delta_1, \ldots, \delta_{N-B}), V(\mathbf{y}^{\star}_{\mathcal{A}(B),\ell}) > \epsilon \right\}.$$

If $V(\mathbf{y}^{\star}_{\mathcal{A}(N)} = \mathbf{y}^{\star}_{\mathcal{A}(B),\ell}) \leq \epsilon$, the $\mathcal{B}_{\mathcal{A}(B),\ell}$ is empty and $\Pr(\mathcal{B}_{\mathcal{A}(B),\ell}) = 0$. On the other hand, if $V(\mathbf{y}^{\star}_{\mathcal{A}(N)} = \mathbf{y}^{\star}_{\mathcal{A}(B),\ell}) > \epsilon$, the $\mathcal{B}_{\mathcal{A}(B),\ell}$ is non-empty, and because the $\mathcal{A}(N)$ in $\mathcal{B}_{\mathcal{A}(B),\ell}$ yields an optimal solution $\mathbf{y}^{\star}_{\mathcal{A}(N)} = \mathbf{y}^{\star}_{\mathcal{A}(B),\ell}$, the $\mathbf{A}^{(\delta)} \mathbf{y}^{\star}_{\mathcal{A}(N)} \preceq \mathbf{b}$ holds for realizations $\delta_1, \ldots, \delta_{N-B}$ in $\mathcal{A}(N) \in \mathcal{B}_{\mathcal{A}(B),\ell}$. Thus, for the latter, the probability that an arbitrary UE realization δ satisfies the constraint $\mathbf{A}^{(\delta)} \mathbf{y}^{\star}_{\mathcal{A}(B),\ell} \preceq \mathbf{b}$ is upper bounded by $1 - \epsilon$, yielding

$$\Pr\left(\mathcal{B}_{\mathcal{A}(B),\ell}\right) \leq (1-\epsilon)^{N-B}, \tag{20}$$

where we use the fact that $\{\delta_i\}_{i=1}^{N-B}$ are independent. It is noteworthy to realize that any realization in $\mathcal{B}$ in (13) belongs to a $\mathcal{B}_{\mathcal{A}(B),l}$ and thereby, $\mathcal{B} = \bigcup_{\forall \mathcal{A}(B),\ell} \mathcal{B}_{\mathcal{A}(B),\ell}$. The $\Pr(\mathcal{B})$ in (14) can be therefore upper-bounded by

$$\Pr(\mathcal{B}) \leq \sum_{\forall \mathcal{A}(B),\ell} \Pr\left(\mathcal{B}_{\mathcal{A}(B),\ell}\right) \leq \binom{K}{B} \binom{B}{B/2} (1-\epsilon)^{N-B},$$

where $\binom{K}{B}$ is the number of different combinations of B elements in Δ. Setting $\binom{K}{B}\binom{B}{B/2}(1-\epsilon)^{N-B} \leq \gamma$ to guarantee the robustness in (14), taking the natural logarithm of both sides, and applying the Stirling's formula [15, (1.13)] to $\ln \binom{K}{B} \approx (K-B) \ln \frac{K}{K-B} + B \ln \frac{K}{B}$ reveals (18). ■

Seen from (18), the $\overline{N}(\epsilon, \gamma)$ grows drastically as either γ or ϵ decrease (i.e., become more robust). For example of $K = 10^6$, $B = 164$, and $(\epsilon, \gamma) = (0.15, 0.1)$, (18) gives $\overline{N}(\epsilon, \gamma) = 9986$. However, slightly lowering (ϵ, γ) to (0.05,0.05) gives $\overline{N}(\epsilon, \gamma) = 31286$. While these bounds are much smaller than the size of Δ ($K = 10^6$), it is still computationally challenging as the resulting constraint matrix

$$\mathbf{A} = \left[(\mathbf{A}^{(\delta_1)})^T, \ldots, (\mathbf{A}^{(\delta_N)})^T \right]^T \in \mathbb{R}^{\sum_{\delta \in \mathcal{A}(N)} U^{(\delta)} \times B}$$

has massive dimensions. As a remedy, a low-complexity sequential search algorithm, based on searching for a small-dimensional substitute for $\mathcal{A}(N)$, is proposed in the next section.

V. Iterative Search Algorithm for BS Deployment

In this section, we devise a low-complexity iterative algorithm solving the problem in (11) with $N = \overline{N}(\epsilon, \gamma)$. The algorithm is based on iteratively solving the following problem

$$\min_{\mathbf{y}} \sum_{b=1}^{B} y_b \quad \text{s.t.: } \mathbf{A}^{(\delta)} \mathbf{y} \preceq \mathbf{b}, \ \forall \delta \in \mathcal{C}, \tag{21}$$

where the size of the set $\mathcal{C}$ is increasing with the iteration.

Specifically, it is initialized with $\mathcal{C} = \{\delta_1\}$, where $\delta_1 \in \mathcal{A}(N)$ in (11), and then recursively adds a $\delta \in \mathcal{A}(N)$ into $\mathcal{C}$ to search for an optimal solution to problem (21). In the first iteration, we obtain a solution $\mathbf{y}^{\star,(1)}_{\mathcal{C}}$ with $\mathcal{C} = \{\delta_1\}$. If there exists a $\delta_2 \in \mathcal{A}(N)$ satisfying $\mathbf{A}^{(\delta_2)} \mathbf{y}^{\star,(1)}_{\mathcal{C}} \not\preceq \mathbf{b}$, $\mathcal{C}$ is updated to $\mathcal{C} = \mathcal{C} \cup \{\delta_2\}$. To efficiently find the solution $\mathbf{y}^{\star,(2)}_{\mathcal{C}}$ with a reduced complexity, we leverage the previous solution $\mathbf{y}^{\star,(1)}_{\mathcal{C}}$ to obtain a feasible solution to problem (21) with the updated $\mathcal{C}$. This can be simply done by sequentially adding new BSs to the existing $\mathbf{y}^{\star,(1)}_{\mathcal{C}}$ to cover the UEs in δ_2 that violate the physical blockage constraint in (2). Taking the found feasible solution as an initial condition of a numerical ILP solver (e.g., Gurobi), the problem (21) at the 2nd iteration can be efficiently and optimally solved, yielding $\mathbf{y}^{\star,(2)}_{\mathcal{C}}$. The above procedure is repeated until the incumbent $\mathbf{y}^{\star,(t)}_{\mathcal{C}}$, where t is the iteration number, is feasible to all elements in $\mathcal{A}(N)$ in (11). Due to the fact that $\mathcal{C} \subset \mathcal{A}(N)$, the $\mathbf{y}^{\star,(t)}_{\mathcal{C}}$ is then the optimal solution to problem (11). The pseudo code of the details in the proposed algorithm is shown in Algorithm 1.

VI. Simulation Studies

We evaluate the proposed mmWave BS deployment technique in the urban geometry in Fig. 1, where the length and width of buildings and the street width are set to $l_{\text{bld}} = 100$ m, $w_{\text{bld},1} = 100$ m, $w_{\text{bld},2} = 40$ m, and $w_{\text{st}} = 20$ m, respectively. The total number of candidate BS locations is $B = 164$. There are $N_{\text{RF}} = 8$ RF chains per BS. According to [12, Corollary 1.1], α and β in (1) are set to be 0.007 and 0.0037, respectively. We set the maximum tolerance levels for the physical and capacity-limited blockage rate to $\zeta^{\text{phy}} = 0.05$ in (2) and $\zeta^{\text{cap}} = 0.02$ in (5). The urban link budget model in 28 GHz bands with transmit power

[4]For an odd B, the right hand side of (19) becomes $\binom{B}{B/2+1/2}$.

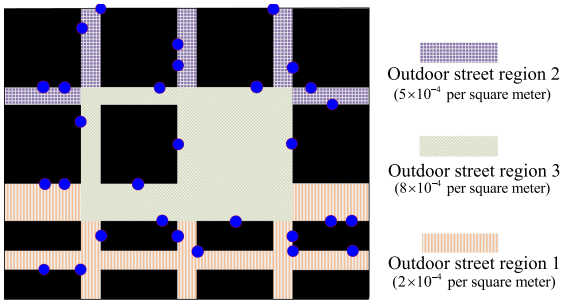

Fig. 2. Optimally deployed 30 BSs under $(\epsilon, \gamma) = (0.05, 0.05)$.

TABLE I
STATISTICS OF ALGORITHM 1

(ϵ, γ)	$(0.15, 0.10)$	$(0.05, 0.05)$
$N = \overline{N}(\epsilon, \gamma)$	9986	31286
$\text{sum}(\mathbf{y}^{\star}_{\mathcal{A}(N)})$	29	30
CPU running time (seconds)	1948	5552
Iteration number	118	158
$V(\mathbf{y}^{\star}_{\mathcal{A}(N)})$	0.071	0.022

Algorithm 1: Iterative Search Algorithm.

1: **Initialize:** $\mathcal{C} = \{\delta_1\}$, $\delta_1 \in \mathcal{A}(N)$, iteration index $t = 1$.
2: Solve problem (21) to obtain a solution $\mathbf{y}_{\mathcal{C}}^{\star,(t)}$.
3: **while** 1 **do**
4: Find a $\delta_{t+1} \in \mathcal{A}(N)$ satisfying $\mathbf{A}^{(\delta_{t+1})}\mathbf{y}_{\mathcal{C}}^{\star,(t)} \not\leq \mathbf{b}$.
5: **if** δ_{t+1} exists **then**
6: Update $\mathcal{C} = \mathcal{C} \bigcup \{\delta_{t+1}\}$.
7: Find a feasible solution to (21) with the updated $\mathcal{C}$, take it as an initialization to solve (21), and obtain $\mathbf{y}_{\mathcal{C}}^{\star,(t+1)}$
8: Update $t = t + 1$.
9: **else**
10: Break
11: **end if**
12: **end while**
13: **return** optimal solution $\mathbf{y}_{\mathcal{C}}^{\star,(t)}$.

30 dBm is considered, which gives the maximum LoS link distance 200 m [13], i.e., $r_{u,b} \leq 200$ m in (1). The UE realization set Δ with $\text{card}(\Delta) = K = 10^6$ is drawn following different homogeneous PPPs in different outdoor street regions as shown in Fig. 2: the active UEs are drawn in the regions $1-3$ with the densities 2×10^{-4}, 5×10^{-4}, and 8×10^{-4} per square meter. In this setting, each UE realization has on average 35 active UEs.

For each (ϵ, γ) in Table I, we set $N = \overline{N}(\epsilon, \gamma)$, based on (18), and sample each $\mathcal{A}(N)$ to formulate problem (11), which is optimally solved by Algorithm 1. For both cases in Table I, the obtained violation probability satisfies $V(\mathbf{y}^{\star}_{\mathcal{A}(N)}) \leq \epsilon$, verifying the proposed scenario sampling theory. It is found in Table I that Algorithm 1 with (0.05,0.05), for instance, converges after 158 iterations and terminates within 5552 seconds of running time. In contrast, instead of using Algorithm 1, directly solving problem (11) for $N = 31286$ leads to memory outage. This is because, with $N = 31286$ and on average 35 UEs in each UE realization, the dimensions of constraint matrix $\mathbf{A}$ for problem (11) become around $(35 \times 31286) \times 164$ ($B = 164$). This is much larger than $(35 \times 158) \times 164$ for Algorithm 1, i.e., at the 158th iteration. The resulting 30 BSs for $(\epsilon, \gamma) = (0.05, 0.05)$ are displayed in Fig. 2.

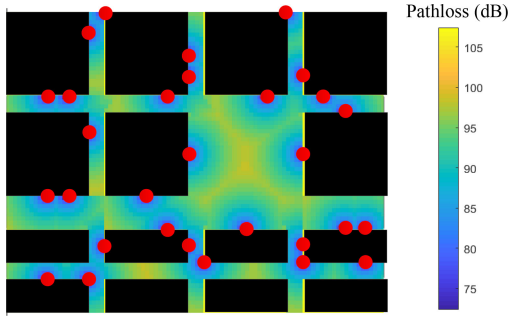

Fig. 3. Pathloss distribution of the BS deployment result in Fig. 2.

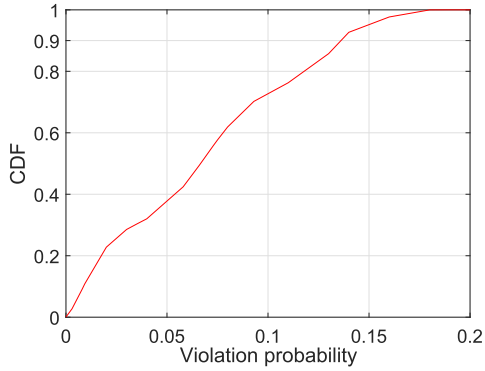

Fig. 4. CDF of violation probability in (12) for $(\epsilon, \gamma) = (0.15, 0.1)$.

Because the region 3 in Fig. 2 has the largest UE density, BSs are mainly deployed at the boundary of each region to concurrently cover the region 3 as well as regions 1 and 2.

In Fig. 3, we visualize the coverage of the deployed BSs in terms of the LoS pathloss measured at 28 GHz [16], which is given by Pathloss $= 61.4 + 20\log10(r)$dB, where r is link distance in meter. For visualization purposes, we partition the streets in Fig. 2 into numerous small square grids with side-length 5 meters. Since a grid can be LoS-visible to multiple BSs, the pathloss of a grid is set to be the minimum pathloss to its LoS-visible BSs in Fig. 2. Seen from Fig. 3, the maximum pathloss of the deployed BSs occurs at the boundary of each cell with the value around 100 dB. This attenuation can be readily compensated for by using the directional transmission in mmWave communications [17].

Fig. 4 displays the cumulative distribution function (CDF) of the violation probability $V(\mathbf{y}^{\star}_{\mathcal{A}(N)})$ in (12) of the proposed approach for $(\epsilon, \gamma) = (0.15, 0.1)$ in Table I. In Fig. 4, the percentage of violation probability larger than $\epsilon = 0.15$ is $0.04 < \gamma = 0.1$, validating the proposed sampling theory. The gap between 0.04 and $\gamma = 0.1$ comes from the fact that the derived bound $\overline{N}(\epsilon, \gamma)$ in (18) is rather loose. For comparison, we consider another minimum-cost BS deployment technique [7] as our benchmark, that is obtained by replacing the constraints in (9) with the d-macro-diversity constraints, i.e., each outdoor location on the streets is covered by at least d BSs. When $d = 4$, the benchmark deploys 31 BSs with violation probability 17%, which needs slightly more BSs but has much worse UE outage performance than the proposed scheme. This is because the optimal solution of the benchmark is independent of the UE realization. The key advantage of the proposed scenario sampling is in its capability of providing UE outage and robustness guarantee, parameterized by (ϵ, γ) and $\overline{N}(\epsilon, \gamma)$.

VII. Conclusion

We proposed a UE outage-guaranteed mmWave BS deployment technique in urban street scenarios, where the random UE distribution is characterized by its numerous measured realizations. To make the formulated large-scale problem solvable, we developed a scenario sampling approach to obtain a small-scale BS deployment problem and optimally solved the problem by proposing an iterative algorithm. The analysis and simulations showed that our proposed scenario sampling can solve the optimization problem with low complexity and achieve the guaranteed UE outage and robustness.

References

[1] H. Ghadikolaei and C. Fischione, "The transitional behavior of interference in millimeter wave networks and its impact on medium access control," *IEEE Trans. Commun.*, vol. 64, no. 2, pp. 723–740, Feb. 2016.

[2] G. Hassana, Y. Liu, G. Hakim, and K. Drissa, "5G base station deployment perspectives in millimeter wave frequencies using meta-heuristic algorithms," *Electronics*, vol. 8, no. 11, Sep. 2019, Art. no. 1318.

[3] M. Dong, T. Kim, J. Wu, and E. W. M. Wong, "Cost-efficient millimeter wave base station deployment in Manhattan-type geometry," *IEEE Access*, vol. 7, pp. 149 959–149 970, Oct. 2019.

[4] Y. Zhang and L. Dai, "Joint optimization of placement and coverage of access points for IEEE 802.11 networks," in *Proc. IEEE Int. Conf. Commun.*, 2020, pp. 1–7.

[5] Y. Wang and Q. Zhu, "Modeling and analysis of small cells based on clustered stochastic geometry," *IEEE Commun. Lett.*, vol. 21, no. 3, pp. 576–579, Mar. 2017.

[6] Y. Lu, H.-W. Hsu, and L.-C. Wang, "Performance model and deployment strategy for mm-Wave multi-cellular systems," in *Proc. 25th Wireless and Opt. Commun. Conf.*, May 2016, pp. 1–4.

[7] N. Palizban, S. Szyszkowicz, and H. Yanikomeroglu, "Automation of millimeter wave network planning for outdoor coverage in dense urban areas using wall-mounted base stations," *IEEE Wireless Commun. Lett.*, vol. 6, no. 2, pp. 206–209, Apr. 2017.

[8] S. Fischer, "Observed time difference of arrival (OTDOA) positioning in 3GPP LTE," Oct. 2019. [Online]. Available: https://www.qualcomm.com/media/documents/files/otdoa-positioning-in-3gp% p-lte.pdf

[9] G. C. Calafiore and M. C. Campi, "The scenario approach to robust control design," *IEEE Trans. Autom. Control*, vol. 51, no. 5, pp. 742–753, May 2006.

[10] W. Zhang, T. Kim, and S. Leung, "A sequential subspace method for millimeter wave MIMO channel estimation," *IEEE Trans. Veh. Technol.*, vol. 69, no. 5, pp. 5355–5368, 2020.

[11] L. Raschkowski, P. Kysti, K. Kusume, and T. Jms, "Deliverable D1.4: METIS channel models," Feb. 2015. [Online]. Available: https://metis2020.com/wp-content/uploads/deliverables/METIS_D1.4_v1.0.p%df

[12] T. Bai, R. Vaze, and R. W. Heath, "Analysis of blockage effects on urban cellular networks," *IEEE Trans. Wireless Commun.*, vol. 13, no. 9, pp. 5070–5083, Sep. 2014.

[13] M. Dong and T. Kim, "Interference analysis for millimeter-wave networks with geometry-dependent first-order reflections," *IEEE Trans. Veh. Technol.*, vol. 67, no. 12, pp. 12 404–12 409, Dec. 2018.

[14] Gurobi Optimization, "Gurobi Optimizer Reference Manual," Oct. 2019. [Online]. Available: https://www.gurobi.com/

[15] D. J. MacKay, *Inform. Theory, Inference, and Learning Algorithms*. Cambridge Univ. Press, U.K., Sep. 2003.

[16] T. S. Rappaport, Y. Xing, G. R. MacCartney, A. F. Molisch, E. Mellios, and J. Zhang, "Overview of millimeter wave communications for fifth-generation (5G) wireless networks—With a focus on propagation models," *IEEE Trans. Antennas Propag.*, vol. 65, no. 12, pp. 6213–6230, 2017.

[17] W. Zhang, T. Kim, D. J. Love, and E. Perrins, "Leveraging the restricted isometry property: Improved low-rank subspace decomposition for hybrid millimeter-wave systems," *IEEE Trans. Commun.*, vol. 66, no. 11, pp. 5814–5827, Nov. 2018.